Three-dimensional modelling of sound absorption in porous asphalt pavement for oblique incident waves

Marieke Bezemer-Krijnen, Ysbrand H. Wijnant, André de Boer
Department of Mechanical Engineering, University of Twente, Enschede, The Netherlands.

Summary
Sound absorption of porous asphalt pavements is an important property when reducing tyre-road noise. A hybrid model has been developed to predict the sound absorption of porous roads. This model is a combination of an analytical analysis of the sound field and a numerical approach, including both the viscothermal effects and the scattering effects. The model provides a description of the three-dimensional sound field in and above the porous asphalt pavement and can be used to predict the absorption coefficient for oblique incident sound waves.

PACS no. 43.20, 43.28, 43.40

1. Introduction

Tyre road noise can be reduced by increasing the sound absorption of the pavement. Properties that influence the sound absorption are for example the porosity, the stone size, the type of bitumen and fillers. The sound absorption and impedance of porous materials can be predicted with ground impedance models. An overview of the different model approaches and models is given by Attenborough et al. [1]. With such models the absorption behaviour of porous pavements can be optimised before construction of the road. However, these models assume that the behaviour of the porous pavement is homogeneous and locally reacting. Therefore, the reflection and scattering of the sound waves on the surface of the pavement and on the stones within the pavement is not accounted for.

In this paper, a numerical model is presented which describes the three-dimensional sound field in and above the porous asphalt pavement and is used to predict the absorption coefficient for oblique incident sound waves. The modelling approach is a combination of an analytical and a finite element approach, including both the viscothermal effects within the pores of the pavement and the scattering effects at the stones in the pavement. Using this modelling approach it is not difficult to model different gradings in multilayered asphalt pavement. Also, the effect of the angle of incidence can be included when modelling the porous asphalt pavement, which is important since a rolling tyre will radiate noise in all directions.

In this paper the ongoing research of this modelling approach is described. In an earlier publication of the authors [2], this approach is introduced for a two-dimensional problem. Here, the approach is extended to a three-dimensional problem. The approach and simulation results for 3 three-dimensional configurations are given in this paper. The developed model can be validated by measurements of the absorption coefficient for oblique incident sound waves using a small microphone array [3].

2. Hybrid modelling approach

A three-dimensional hybrid model is developed which predicts the sound field in and above nonlocally reacting porous materials and which includes viscothermal and scattering effects. In this research is focused on porous asphalt pavements.

The approach used for this model is shown in Figure 1. It is a combination between the analytical solution of the sound field in two mediums with acoustically hard backing, shown at the top left of Figure 1, and a numerical approach, where the scattering of the sound waves is included, as shown on the top right side of Figure 1. The total pressure field is then given by the combination of the analytical solution and the finite element solution, shown at the bottom of Figure 1.

The analytical solution is derived for the sound field in two mediums, where one medium represents air and the other medium is an air layer including energy dissipation by viscous and thermal effects. The second medium has an acoustically hard backing. The sound

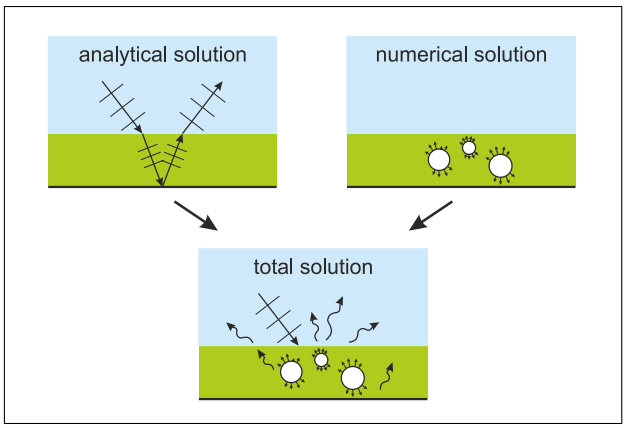

Figure 1. Modelling approach.

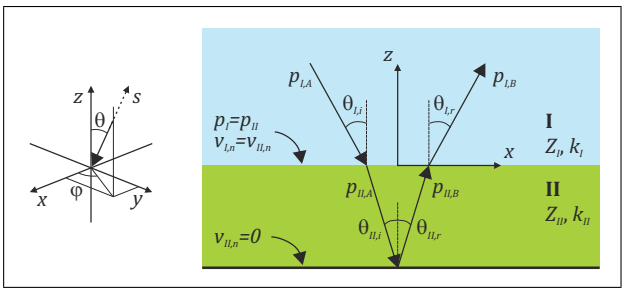

Figure 2. Directions, polar angle θ and azimuthal angle φ (left) and 2D view of boundary conditions for analytical solution (right).

field is derived for an incoming wave field with an arbitrary angle of incidence, which will be partly reflected at the interface with the second medium and partly absorbed by the second medium, due to the viscothermal dissipation of energy. At the acoustically hard backing at the bottom of the second medium the remaining sound waves are reflected and again partly absorbed in medium II, partly reflected at the interface with medium I and partly transmitted back into medium I.

The acoustic properties of a porous asphalt pavement can be determined with a microstructural ground impedance model. In these models the acoustic properties of the air within the (small) pores of the porous asphalt pavement are derived from analytical descriptions of a fluid flowing through pores with a simple geometry and uniform cross-section, like cylindrical tubes. Most models include shape factors to describe the influence of the pore shape on the thermal and viscous effects. The properties of an individual pore are used to find a generalized model for the porous material, for example by using the porosity. Various microstructural models are available, [4], [5], [6].

A similar approach is used in the low reduced frequency (LRF) model [7], [8], which is used in this modelling approach to estimate the acoustic properties of the air within the pores of the asphalt pavement. However, the acoustic properties of the air inside the individual pore are directly used for the second medium, instead of deriving an impedance representative for a medium with a certain porosity, such that the impedance homogeneous over this layer. Thus, in the hybrid modelling approach, the acoustic properties belonging to a single pore are used for the analytical solution and for the numerical model. The correct porosity is obtained only in the combination with the numerical model. This is also a homogenisation of the acoustic properties, but since this approach is combined with a scattering problem, the total approach is not an homogenisation. And therefore, it is possible to study the sound absorption for oblique incidence and the influence of different gradings in multilayered asphalt pavement.

An other advantage of this approach is that the viscothermal effects are included in the properties of the medium, by means of a complex wave number, speed of sound and impedance, and not as special viscothermal finite elements which have large computational cost.

The numerical models are made with the multiphysics package Comsol, version 4.4, in combination with Matlab, version 2013a.

In Section 2.1 the analytical solution and in Section 2.2 the numerical solution are described and applied to example cases. The coupled numerical model is described in Section 2.3.

2.1. Analytical solution including viscothermal effects

An incoming sound wave including reflection and dissipation of energy by the viscothermal effects can be described by the sound pressure and particle velocity. The pressure in domain I (see Figure 2) is given by p_{I}

$$p_{\mathrm{I}} = A_{\mathrm{I}} e^{ik_{\mathrm{I}} s_{\mathrm{I}}} + B_{\mathrm{I}} e^{-ik_{\mathrm{I}} s_{\mathrm{I}}}, \tag{1}$$

and for domain II by p_{II}

$$p_{\mathrm{II}} = A_{\mathrm{II}} e^{ik_{\mathrm{II}} s_{\mathrm{II}}} + B_{\mathrm{II}} e^{-ik_{\mathrm{II}} s_{\mathrm{II}}}, \tag{2}$$

where, A_l and B_l are the complex amplitudes of respectively the incident and reflected waves, l indicates the domain and s is a spatial coordinate defined by the position, the polar angle of incidence θ_l and azimuthal angle of incidence φ_l:

$$s_l = x \sin\theta_l \cos\varphi_l + y \sin\theta_l \sin\varphi_l + z \cos\theta_l. \tag{3}$$

It is assumed that $\theta_l = \theta_{l,i} = -\theta_{l,r}$ and $\varphi_l = \varphi_{l,i} = \varphi_{l,r}$.

The particle velocity in the direction normal to the the interface between domain I and domain II is given by $v_{\mathrm{I},n}$ for domain I:

$$v_{\mathrm{I},n} = \frac{-A_{\mathrm{I}} \cos\theta_{\mathrm{I}}}{Z_{\mathrm{I}}} e^{ik_{\mathrm{I}} s_{\mathrm{I}}} + \frac{B_{\mathrm{I}} \cos\theta_{\mathrm{I}}}{Z_{\mathrm{I}}} e^{-ik_{\mathrm{I}} s_{\mathrm{I}}}, \tag{4}$$

and by $v_{\mathrm{II},n}$ for domain II:

$$v_{\mathrm{II},n} = \frac{-A_{\mathrm{II}} \cos\theta_{\mathrm{II}}}{Z_{\mathrm{II}}} e^{ik_{\mathrm{II}} s_{\mathrm{II}}} + \frac{B_{\mathrm{II}} \cos\theta_{\mathrm{II}}}{Z_{\mathrm{II}}} e^{-ik_{\mathrm{II}} s_{\mathrm{II}s}}. \tag{5}$$

2.1.1. Boundary conditions

The analytical solution is found using the continuity of the pressure and the particle velocity in normal direction at $z = 0$ and the sound hard boundary at $z = -d$, where d is the thickness of medium II.

$$p_{\mathrm{I}}|_{z=0} = p_{\mathrm{II}}|_{z=0} \tag{6}$$

$$v_{\mathrm{I},n}|_{z=0} = v_{\mathrm{II},n}|_{z=0} \tag{7}$$

$$v_{\mathrm{II},n}|_{z=-d} = 0 \tag{8}$$

The boundary conditions are shown on the right side of Figure 2. Solving the system for an incident wave of unit amplitude, $A_1 = 1$, yields:

$$B_{\mathrm{I}} = A_{\mathrm{I}} \frac{Z_{\mathrm{II}} \cos\theta_{\mathrm{I}} \left(1 + e^{\xi}\right) - Z_{\mathrm{I}} \cos\theta_{\mathrm{II}} \left(1 - e^{\xi}\right)}{Z_{\mathrm{II}} \cos\theta_{\mathrm{I}} \left(1 + e^{\xi}\right) + Z_{I} \cos\theta_{\mathrm{II}} \left(1 - e^{\xi}\right)} \tag{9}$$

$$A_{\mathrm{II}} = 2A_{\mathrm{I}} \frac{Z_{\mathrm{II}} \cos\theta_{\mathrm{I}}}{Z_{\mathrm{II}} \cos\theta_{\mathrm{I}} \left(1 + e^{\xi}\right) + Z_{\mathrm{I}} \cos\theta_{\mathrm{II}} \left(1 - e^{\xi}\right)} \tag{10}$$

$$B_{\mathrm{II}} = A_{\mathrm{II}} e^{\xi} \tag{11}$$

where

$$e^{\xi} = e^{-2ik_{\mathrm{II}} d \cos\theta_{\mathrm{II}}} \tag{12}$$

The boundary conditions and the solution procedure are described in more detail in [2].

2.1.2. Example

The equations for the pressure and particle velocity are implemented in a numerical model. To demonstrate the analytical solution, an example model, called model A, has been built. In this model the stones are not included and the impedance of the second medium is derived from the impedance for a single cylindrical pore, Z_{pore}, using the porosity Ω of the porous layer, [7]:

$$Z_{\mathrm{II}} = \frac{Z_{\mathrm{pore}}}{\Omega}, \tag{13}$$

where Z_{II} is the impedance of medium II. The impedance of the single pore is found using the LRF model for a cylindrical pore with the dimensions and porosity listed in Table I. The impedance used in the analytical model is not frequency dependent. This value is the averaged impedance value over the range of frequencies used in the simulations. Note that the LRF model returns a frequency dependent impedance.

The three-dimensional model is shown in Figure 3 and consists of a half sphere representing the air in medium I and a cylindrical layer representing the porous material in medium II. Both layers are enclosed by perfectly matched layers (PML), such that pressure waves entering these layers are completely absorbed without reflections. PML are introduced by Berenger [9] for the application of electromagnetic waves.

Table I. Parameters for LRF model of example model A.

Property	Value
equivalent radius tube, R_{tube} $[mm]$	3.5
length pore, L_{pore} $[mm]$	75
impedance pore, Z_{pore} $[kg/\left(m^2 s\right)]$	$407 + 6i$
porosity, Ω [-]	0.44

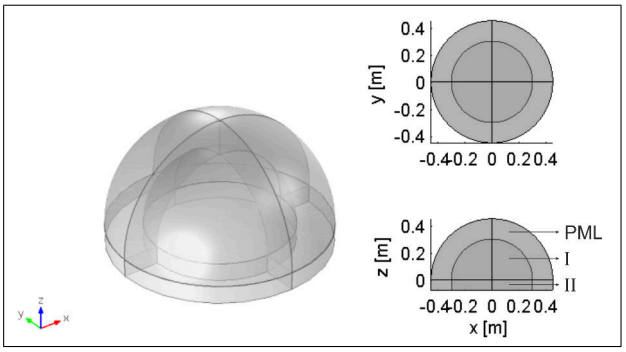

Figure 3. Example model A with 2 layers enclosed by perfectly matched layers.

Table II. Properties of example model A.

Property	Value
speed of sound in medium I $[m/s]$	343
speed of sound in medium II $[m/s]$	$768 + 11i$
impedance in medium I $[kg/\left(m^2 s\right)]$	413
impedance in medium II $[kg/\left(m^2 s\right)]$	$925 + 13i$
height medium II $[m]$	75

The analytical solution of the total pressure field is projected onto this model, shown in Figure 4. This is the solution of the incident pressure field, shown in Figure 5, using the model parameters listed in Table II. The incident pressure field is not continuous at the interface of domain I and II, since the complex amplitude A_{II} is defined as the sum of all incident pressure waves in medium II. Note that the solution is given for the boundary condition where the sum of the amplitudes of all incident and all reflected waves is continuous over this interface (Eq. 6).

2.2. Scattering problem

The second part of the hybrid modelling approach is the scattering problem, as shown on the top right part of Figure 1. This problem is solved using the finite element method.

The three-dimensional numerical model used to solve the scattering problem consists of a half sphere representing the air in medium I and a box containing stacked spheres representing the individual stones in the asphalt concrete, as shown in Figure 6.

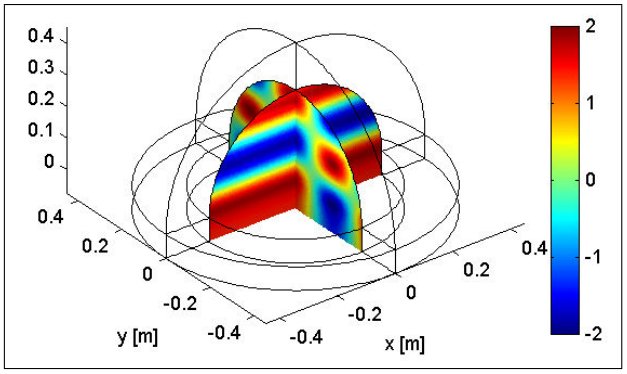

Figure 4. Total pressure field for model A ($f = 1600Hz$, $\theta = 35°$ and $\varphi = 90°$).

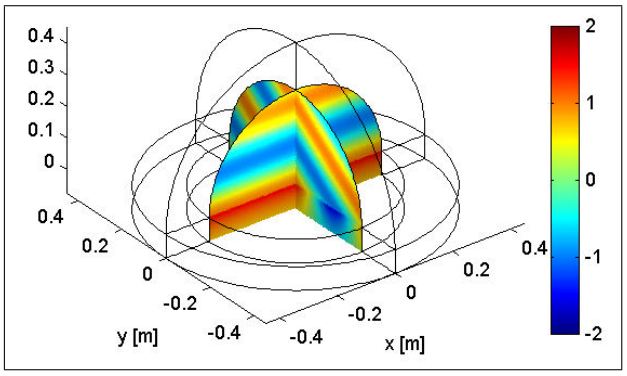

Figure 5. Incident pressure field for model A ($f = 1600Hz$, $\theta = 35°$ and $\varphi = 90°$).

With this finite element model the scattering of the sound waves on the stone structure and the box itself is solved. This is implemented by applying the analytical solution of the particle velocity, as given in Eq. 5, on the boundaries of the stacked spheres and the enclosing box. The total particle velocity in normal direction, consisting of the analytical particle velocity of the incoming and the reflected waves ($v_{\mathrm{II},n}$) and the particle velocity of the scattered waves ($v_{scat,n}$), is set to zero at the boundaries.

2.2.1. Stacked spheres

The stones in the porous pavement are represented in this model by a structure of spheres. The structure of the stacked spheres is based on the face-centered cubic system, since this structure has a low porosity and is therefore more realistic.

In the future more research will be done to optimise this structure for the sound absorption and to find a structure more similar to the stone structures found in real asphalt pavement.

2.2.2. Example

Model B, shown in Figure 6, can be used to demonstrate the scattering approach. The model consists of a half sphere representing the air and a structure of stones within a rectangular box. The parameters of model B are given in Table III, where N_x, N_y and N_z denote the number of spheres in, respectively, x-direction, y-direction and z-direction.

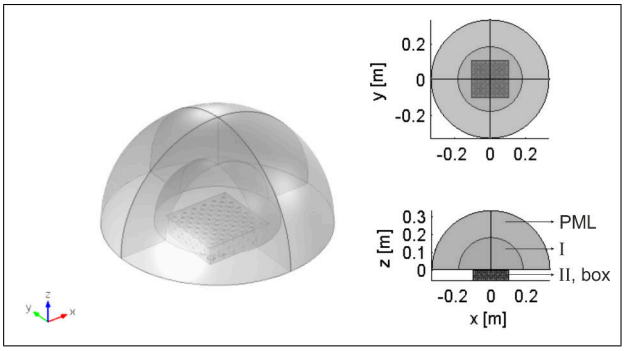

Figure 6. Geometry of the three-dimensional model with stone structure (example model B).

Table III. Parameters of stacked sphere structures of example models.

Property	Model B	Model C
radius spheres $[mm]$	12	8
height porous layer $[mm]$	61	65
porosity [-]	0.44	0.42
N_x [-]	11	16
N_y [-]	11	16
N_z [-]	3	5

Table IV. Properties of medium II of example models.

Property	Model B	Model C
speed of sound $[m/s]$	$338 + 5i$	$336 + 7i$
impedance $[kg/\left(m^2 s\right)]$	$407 + 6i$	$405 + 8i$
porosity [-]	0.44	0.42

The acoustic properties of medium I are the same as for air and the half sphere is circumscribed by perfectly matched layers. The edges of the box representing the porous asphalt concrete are rounded, to avoid numerical problems. Also, some problems regarding the mesh were encountered, these were solved by modelling a small gap between the stones in the sphere structure and by reducing the radius of the half sphere containing medium I. The acoustic properties of medium II are summarized in Table IV.

The scattering problem is solved for an angle of incidence of $\theta = 35°$ and $\varphi = 150°$. The scattered pressure field for a frequency of $1150Hz$ is shown in Figure 7.

2.3. Coupled numerical model

In the hybrid modelling approach the analytical solution is combined with the solution of the scattering problem in a coupled numerical model. This is done

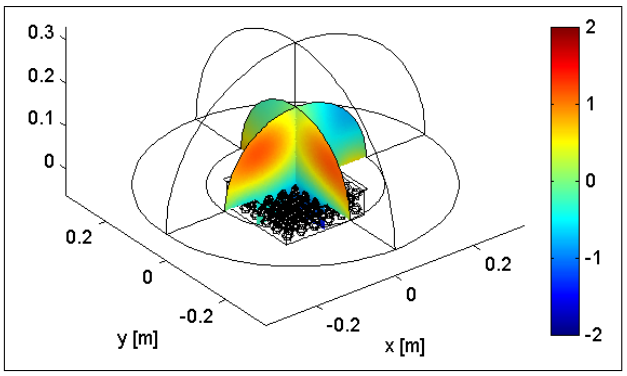

Figure 7. Scattered pressure field for model B ($f = 1150Hz$, $\theta = 35°$ and $\varphi = 150°$).

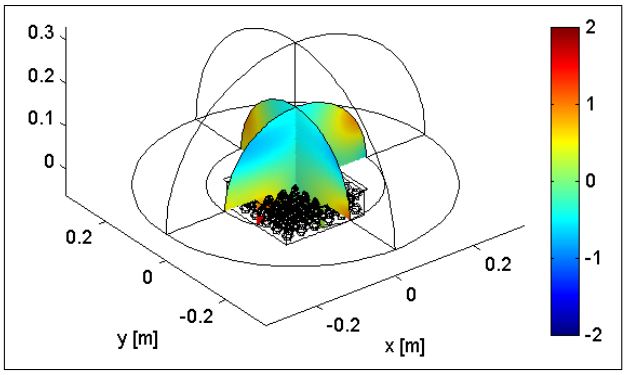

Figure 8. Total pressure field for model B ($f = 1150Hz$, $\theta = 35°$ and $\varphi = 150°$).

by adding the analytical solution to the numerical solution of the scattering problem, both for the same analytical incident pressure.

2.3.1. Example

The solution of the total pressure field of model B is obtained by adding the analytical solution of the incident and reflected pressure field to the numerical solution of the scattered pressure field. The total pressure field is shown in Figure 8.

A third model is built using the parameters for model C is given in Table III. The spheres in model C have a diameter of $16mm$. The acoustic properties are listed in Table IV. Because, compared to model B, the diameter of the spheres is smaller and the height of the porous layer larger, the LRF model to find these properties is based on a single pore with a smaller radius and a longer tube length. Therefore, compared to the properties of model B (Table IV), it is as expected that the properties of model C contain a larger imaginary part, since this indicates more viscothermal behaviour.

3. Sound absorption coefficient

The coupled model can be used to predict the sound absorption coefficient for a certain frequency and angle of incidence. The area averaged absorption coefficient α over the interface S between domain I and II is defined as the fraction of the time-averaged incident sound power W_{in} that is absorbed by this area:

$$\alpha = \frac{W_{in} - W_{refl}}{W_{in}}, \tag{14}$$

where W_{in} and W_{refl} are, respectively, the time-averaged incident and reflected sound power at S, as described by [10].

The incident and reflected power cannot be determined directly, but can be described in terms of the complex amplitudes A and B if the sound field can be described locally by plane waves. The complex amplitudes are derived from the 'measured' complex pressure p and complex particle velocity in normal direction v_n:

$$A = \frac{1}{2}\left(p + \rho c v_n\right), \tag{15}$$

and

$$B = \frac{1}{2}\left(p - \rho c v_n\right). \tag{16}$$

The incident and reflected intensity are given by:

$$I_{in} = \frac{A\overline{A}}{2\rho c}, \tag{17}$$

and

$$I_{refl} = \frac{B\overline{B}}{2\rho c}. \tag{18}$$

where $\overline{A}$ denotes the complex conjugate of A. The incident and reflected power can be obtained by integration of the incident and reflected intensity over the interface S.

3.1. Absorption coefficient for model B

Multiple simulations are performed with model B to determine the absorption coefficient for a range of frequencies and different angles of incidence. In Figure 9 the absorption coefficient for model B is shown for three combinations of the polar and azimuthal angle of incidence. Also, the analytical solution for normal incidence using the LRF model with the parameters listed in Table I is shown in this figure. These results show that up to $f = 1300Hz$, the absorption behaviour of model B (for normal incidence) follows the absorption coefficient given by the LRF model. For higher frequencies, the absorption coefficient of model B is lower, which can be caused by the scattering effects.

The two simulations for oblique incidence show higher absorption coefficients for the low frequencies than would be expected for locally reacting surfaces, which indicates that the stone structure has indeed an influence on the absorption behaviour for oblique incidence.

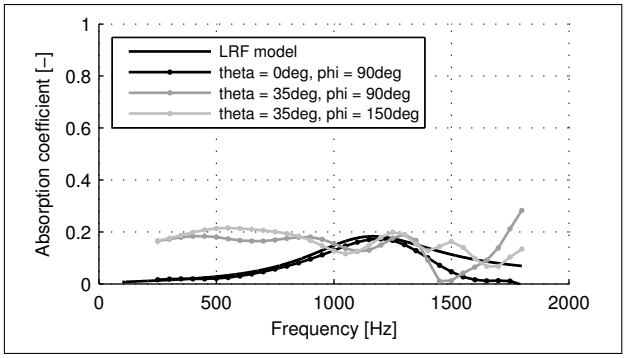

Figure 9. Absorption coefficient for model B.

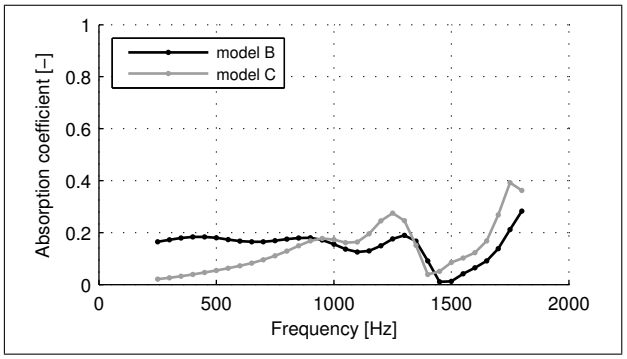

Figure 10. Absorption coefficient for oblique incidence ($\theta = 35°$ and $\varphi = 90°$).

3.2. Absorption coefficient for oblique incidence

The absorption coefficient is also given for model C. In Figure 10 the absorption coefficient is shown for $\theta = 35°$ and $\varphi = 90°$. In this figure can be seen that a smaller diameter of the stones (model C), gives a smaller absorption coefficient for low frequencies, but a larger absorption coefficient for higher frequencies. The results show that this modelling approach can be used to optimise the sound absorption of different structures.

4. Conclusions and future work

In this paper a hybrid modelling approach is described, which can be used to predict the sound absorption coefficient for porous materials at oblique incidence. In this paper, we focus on the application of porous asphalt concrete. With this approach the sound absorbing properties for oblique incidence of porous asphalt pavement based on geometric properties can be predicted. In the future, the geometry of the stone structure will be changed to a more realistic structure and this will optimised for better sound absorbing properties.

The modelling approach is explained and demonstrated for some example models. It is shown that the absorption coefficient for normal incidence follows the absorption coefficient predicted by a microstructural impedance model and that the structure of the stones has influence on the absorption coefficient. In the future, the hybrid modelling approach will be validated with an experimental setup. Also, possibilities to reduce the amount of elements in the three-dimensional model will be studied.

Acknowledgement

This project is carried out in the framework of the innovation program 'GO Gebundelde Innovatiekracht', and funded by the 'European Regional Development Fund', 'Regio Twente' and 'Provincie Overijssel'. The project partners Apollo Tyres Global R&D, University of Twente (Tire-Road Consortium), Reef Infra, STEMMER IMAGING and the Provincie Gelderland are gratefully acknowledged.

References

[1] K. Attenborough, I. Bashir, S. Taherzadeh: Outdoor ground impedance models. J. Acoust. Soc. Am., Vol. 129, 2806-2819 (2011).

[2] M. Bezemer-Krijnen, Y. H. Wijnant, A. de Boer: Modelling absorption in porous asphalt concrete for oblique incident sound waves. Proceedings of ISMA2014 including USD2014 (2014), 1723-1730.

[3] M. Bezemer-Krijnen, Y. H. Wijnant, A. de Boer, D. Bekke: On the sound absorption coefficient of porous asphalt pavements for oblique incident sound waves. Inter-noise 2014 (2014).

[4] J. Allard, N. Atalla: Propagation of Sound in Porous Media: Modelling Sound Absorbing Materials 2e. John Wiley & Sons (2009).

[5] K. Attenborough: Acoustical characteristics of rigid fibrous absorbents and granular materials. J. Acoust. Soc. Am., Vol. 73, 785-799 (1983).

[6] Y. Champoux, M. R. Stinson: On acoustical models for sound propagation in rigid frame porous materials and the influence of shape factors. J. Acoust. Soc. Am., Vol. 92, 1120-1131 (1992).

[7] F. J. M. van der Eerden: Noise reduction with coupled prismatic tubes. University of Twente (2000).

[8] M. H. C. Hannink: Acoustic resonators for the reduction of sound radiation and transmission. University of Twente (2007).

[9] J.-P. Berenger: A perfectly matched layer for the absorption of electromagnetic waves. J. Computat. Phys., Vol. 114, 185-200 (1994).

[10] Y. H. Wijnant, E. R. Kuipers, A. de Boer: Development and application of a new method for the in-situ measurement of sound absorption. Proceeding of ISMA2010 including USD2010, 109-122 (2014).